EXPERIMENTAL STUDY OF BUOYANT–THERMOCAPILLARY CONVECTION IN A RECTANGULAR CAVITY

Manfred. G. Braunsfurth and George. M. Homsy
Department of Chemical Engineering,
Stanford University, Stanford, CA 94305

ABSTRACT

The problem of buoyant–thermocapillary convection in cavities is governed by a relatively large number of nondimensional parameters, and there is consequently a large number of different types of flow that can be found in this system. Previous results give disjoint glimpses of a wide variety of qualitatively and quantitatively different results in widely different parts of parameter space. In this study, we report experiments on the primary and secondary instabilities in a geometry with equal aspect ratios in the range from 1 to 8 in both the direction along and perpendicular to the applied temperature gradient. We thus complement previous work which mostly involved either fluid layers of large extent in both directions, or consisted of investigations of strictly two-dimensional disturbances. We observe the primary transition from an essentially two-dimensional flow to steady three-dimensional longitudinal rolls. The critical Marangoni number is found to depend on the aspect ratios of the system, and varies from 4.6×10^5 at aspect ratio 2.0 to 5.5×10^4 at aspect ratio 3.5. Further, we have investigated the stability of the three-dimensional flow at larger Marangoni numbers, and find a novel oscillatory flow at critical Marangoni numbers of the order of 6×10^5. We suggest possible mechanisms which give rise to the oscillation, and find that it is expected to be a relaxation type oscillation.

INTRODUCTION

Buoyant–thermocapillary convection occurs in a variety of different applications, including crystal growth. We choose to study buoyant–thermocapillary convection in a simplified geometry and under carefully controlled experimental conditions, where the link between the observed dynamics and the underlying mechanisms can be made. The geometry of the system considered in this study is shown schematically in figure 1. A horizontal temperature gradient is applied by heating and cooling two opposite sidewalls. The remaining two sidewalls and the bottom are taken to be rigid and insulating, and the top surface of the fluid is free. There are two physical mechanisms which drive fluid flow in this system, buoyancy and thermocapillarity. For fluids with surface tension decreasing with increasing temperature, these mechanisms reinforce each other to drive the convection, but with differing scaling dependence (see Carpenter & Homsy, ref. 1).

The system is characterized by a set of nondimensional parameters, which are the aspect ratios $A_x=\frac{d}{h}$, $A_y=\frac{w}{h}$, the Marangoni number $Ma=\frac{\gamma_T \Delta T d}{\mu\kappa}$, the Raleigh number $Ra=\frac{g\alpha\Delta T h^3}{\nu\kappa}$, the Prandtl number $Pr=\frac{\nu}{\kappa}$, the Capillary number $Ca=\frac{\gamma_T \Delta T}{\gamma}$, and the dynamic Bond number $G=\frac{RaA_x}{Ma}=\frac{g\alpha\rho h^2}{\gamma_T}$. The dynamic Bond number G, while not independent of these groups, is often used as a measure of the relative strength of thermocapillarity to buoyancy driving forces. Finally, there is the contact angle of the fluid with the wall, which is given by the contact angles appropriate for acetone on glass and acetone on copper, and no attempt was made to change these values.

The results of previous studies give disjoint glimpses of a wide variety of qualitatively and quantitatively different results in widely different parts of parameter space. Four different transitions have been seen: from a two-dimensional steady single-cellular flow to (i) steady two-dimensional transverse rolls, (ii) to two-dimensional oscillatory rolls, (iii) to a three-dimensional flow of longitudinal rolls, (iv) to three-dimensional oblique rolls. In this study, we consider a container with equal values for the aspect ratios A_x and

A_y in the range of 1 to 8. This choice of aspect ratios will allow us to complement previous studies. On the one hand, we are considering a system with a moderate aspect ratio A_x, similar to the ones studied by Peltier & Biringen, Xu, Mundrane & Zebib, Schwabe, Moeller, Schneider, & Scharmann, and by Villers & Platten (refs. 2 to 5). On the other hand, due to the fact that $A_x=A_y$ we are not restricting the system to only transverse modes of instabilities, in contrast to those studies. The geometry will also allow fully three-dimensional flows, such as the ones considered by for example Gillon & Homsy and by Mundrane & Zebib (refs. 6, 7). Our results in fact indicate a first instability to longitudinal rolls, as seen by Gillon & Homsy and by Mundrane & Zebib, and we investigate the dependence of the critical Marangoni number for this transition on the aspect ratios. A further aim of our study is to investigate the stability of the longitudinal rolls, and to identify the mechanisms by which time dependence occurs in this flow.

EXPERIMENTAL SETUP

The working section of the experiment is constructed from pieces of glass and two copper blocks, bonded together using silicone rubber sealant, as this is resistant to acetone. The resulting chamber has a width perpendicular to the applied temperature gradient of 10.18 mm ± 0.1 mm, and a length along the temperature gradient of 10.61 mm ± 0.06 mm. The top of the chamber is covered with another piece of glass and a silicone rubber seal, to limit evaporation of the acetone. The thermal conductivity of copper is 400 $W\ m^{-1}K^{-1}$, which is 3 orders of magnitude better than that of acetone, which is 0.16 $W\ m^{-1}K^{-1}$. This ensures a uniform temperature over the whole of the copper side walls. The chamber is insulated from the surroundings, and the temperature stability of the fluid inside the apparatus is measured to be better than ± 0.05 K over the period of a day.

Measurements of the fluid flow are performed using small tracer particles suspended in the fluid. The tracer particles are illuminated by a light sheet, which is provided by a slide projector. The fluid motion can hence be observed either with the eye using a traveling telescope, or can be recorded for later analysis using a CCD camera and high resolution video recorder. In order to obtain quantitative measurements of velocity we employ a particle tracking velocimetry algorithm which was specifically developed for the present setup.

The fluid used in the experiments is acetone. Two experimental parameters were changed between different observations of the flow, the fluid height, and the temperature difference between the side walls. The physical properties of acetone at 14°C lead to the following expressions for the nondimensional groups, $Pr = 4.44$, $Ra = 3.4\times10^{11}\ K^{-1}m^{-3} \times \Delta T\ h^3$, $Ma = 4.00\times10^{4}\ K^{-1} \times \Delta T$, and $G = 9.03\times10^{4}\ m^{-2} \times h^2$. It is important to note that by varying only two experimental parameters, we are always on one particular two-dimensional sub-section of a higher-dimensional parameter space. The aspect ratios in the experiment cover a range from 1 to 8, with an associated range in G from 4 to 0.17. The Marangoni number can be varied between 0 and 8.2×10^5, and the Rayleigh number can cover a range from 0 to 7.1×10^5.

STEADY FLOWS

At small applied temperature differences, i.e. small Marangoni number and small Rayleigh number, the convective flow is essentially two-dimensional. An example of the velocity field for aspect ratio $A_x=1.81$, Marangoni number $Ma=7.67\times10^4$, Rayleigh number $Ra=1.31\times10^5$, and thus $G=3.10$ is shown in figure 2. We observe a single closed convection circulation, rising at the hot wall and hot fluid flowing on the top half of the container towards the cold wall, where the fluid sinks, and flows back along the bottom, thus closing the loop.

A transition from the two-dimensional flow to a steady three-dimensional flow is observed when the temperature difference is increased. The velocity field on the center section of the flow at an aspect ratio of $A_x=2.35$, Marangoni number $Ma=3.44\times10^5$, and Rayleigh number $Ra=2.71\times10^5$ is shown in figure 3. In this case, we see evidence of three-dimensional flow. In the top left corner of the flow domain, at the top of the cold wall, we see that fluid flows into the center plane from regions outside the plane of view. Somewhat surprisingly, this fluid is driven against the expected direction of both the buoyancy forces and of surface tension effects. Where this fluid meets with the main circulation, the velocity components in the plane of the section goes to zero, and here fluid is leaving the center plane. The velocity field was found to be symmetric with respect to reflection about the center plane of the container, and suggests a circulation in the form of two counter-rotating eddies in the plane perpendicular to the temperature gradient. These circulations have

upwelling flow at the sides of the container, and downwelling flow at the center. This type of flow has been observed previously by Gillon & Homsy, and by Mundrane & Zebib (refs. 6, 7).

In figure 4 we show the critical Marangoni number for the onset of the three-dimensional flow as a function of the aspect ratio A_x. The points drawn as triangles represent combinations of the experimental parameters where the flow was found to be two-dimensional in nature, and the circles represent points where the flow is three-dimensional. The line separating the two-dimensional flow and the three-dimensional flow in this aspect ratio – Marangoni number projection lies along $Ma \approx 10^6 - 2.7\times10^5\ A_x$.

OSCILLATORY FLOW

Above Marangoni numbers of 7×10^5 we observe the onset of a novel oscillatory flow, representing a secondary instability of the fully three-dimensional flow described in the last section. As the Marangoni number is increased beyond the onset of the three-dimensional flow, the region in the center section where the fluid is driven in the direction opposite to the expected direction of buoyancy and surface tension forces grows in size, until it fills as much as half of the center section. This is a typical base flow, on which the new oscillatory flow develops in a two-step process, as we will describe next. Upon further increase of the Marangoni number, a small but fast, steady eddy forms in the top right corner, at the top edge of the hot wall. This eddy rotates in the same direction as the main circulation of the convective flow. For example, at an aspect ratio of $A_x=3.56$, the eddy is at first steady and confined to a small region of typical size less than 0.5 mm close to the hot wall. With an increase in Marangoni number from $Ma=6.70\times10^5$ where it first becomes observable to $Ma=6.79\times10^5$, it grows to a typical size of 1.2 mm, with characteristic fluid speeds of 2 mm s^{-1}. A further increase in the Marangoni number to $Ma=6.81\times10^5$ results in the onset of an oscillation of the eddy, during which it begins to oscillate in both size and strength. This scenario is typical for the onset of oscillation at all the aspect ratios considered. The strength of the eddy and the amplitude of its oscillation is largest in the center section of the container, and it diminishes towards the sidewalls in a fashion which is symmetric with respect to reflection about the center plane.

The critical curve of the onset of oscillation in parameter space is shown in figure 4. The circles in figure 4 denote the parameter combinations where the flow was found to be three-dimensional and steady, and the crosses indicate time-dependent flow. At small aspect ratios, the critical Marangoni number for the onset of oscillation is around $Ma_c=7\times10^5$. At an aspect ratio of $A_x=4.5$ we see a sharp drop in the critical Marangoni number, to a value of $Ma_c=5.3\times10^5$, followed by a smooth rise to $Ma_c=6.6\times10^5$ at an aspect ratio of $A_x=7$. The frequency of the oscillation is around 0.7 Hz.

To understand the onset of oscillations, we consider mechanisms in which small disturbances would amplify themselves, and the system would be unstable. We can state that the total temperature difference across the container is constant, since this is applied externally. Thus, the total amount of driving due to surface tension gradients is constant when integrated over the whole length of the container. If now for some reason there is a small temperature fluctuation in the region of the eddy increasing the temperature gradient and leading it to grow, there would be an associated reduction in surface driving in the rest of the flow. In the remainder of the center plane of the flow, the fluid is propelled against the driving due to surface tension forces, and thus a reduction in surface tension forces in this region would be associated with an increase in the flow from the cold wall to the stagnation point. This would increase the temperature gradient across the eddy, and thus lead it to grow further. This argument can also be lead to show that a reduction in size would amplify itself, and is a mechanism for positive feedback, which can provide the driving for an oscillation. Once the eddy grows large on the other hand, there will be stronger advection of heat from the hot wall through the eddy to the stagnation point, thus lowering the temperature gradient and reducing the driving. In addition, when the eddy becomes large, the stagnation point moves away from the hot wall, and thus the local temperature gradient decreases, and the eddy will no longer be able to sustain itself. This scenario bears some similarity to the one described by Kayser & Berg (ref. 8) for the case of convection due to solute concentration gradients. If we assume that the lifetime of the eddy or the period of the oscillation is determined by the advection of heat through the eddy, we can make an estimate of the time scale of such a mechanism. This is the transit time of fluid through the eddy multiplied by the Peclet number to the half power, which is of the order of 2 s, and compares favorably with the frequency of the oscillation, which is of the order of 1 Hz.

CONCLUSIONS

We have investigated experimentally the primary and secondary mechanisms of instability in buoyant–thermocapillary convection, in a rectangular configuration with equal length and width. In this system, we have observed the transition from an essentially two-dimensional flow at small Marangoni numbers to a steady, three-dimensional flow as seen previously by Gillon & Homsy and by Mundrane & Zebib (refs. 6, 7). In addition, we traced the aspect ratio dependence of the critical Marangoni number, and found a strong decrease of the critical Ma with an increase in the aspect ratio. In view of the results of Peltier & Biringen and Xu, Mundrane & Zebib (refs. 2, 3), which find a lower critical aspect ratio for the onset of two-dimensional steady rolls, we speculate that our system becomes three-dimensional before the expected onset of two-dimensional rolls, and that we hence never observe those.

We have further investigated the stability of the three-dimensional flow at larger Marangoni numbers, and have observed a transition to oscillatory behavior. Oscillation takes place in a small confined region, and is driven by the strongly developed three-dimensional flow. We were able to suggest the underlying physical mechanism which gives rise to the oscillation, which consists of a positive feedback mechanism leading the eddy to grow, and a mechanisms by which the eddy eventually destroys itself. This scenario is consistent with a relaxation type oscillation. The appearance of the oscillation may be localized to a section of the three-dimensional cellular flow structure, and may well be very sensitive to the value of the contact angle of the fluid with the wall.

ACKNOWLEDGMENTS

We wish to acknowledge the support of NASA through Contract No. NAG-3-1475.

REFERENCES

1. B. M. Carpenter, G. M. Homsy, "Combined buoyant–thermocapillary flow in a cavity", J. Fluid Mech. **207**, (1989), pp. 121–132.
2. L. J. Peltier, S. Biringen, "Time-dependent thermocapillary convection in a rectangular cavity: numerical results for a moderate Prandtl number fluid", J. Fluid Mech. **257**, (1993), pp. 339–357.
3. J. Xu, M. Mundrane, A. Zebib, personal communication, (1995).
4. D. Schwabe, U. Moeller, J. Schneider, A. Scharmann, "Instabilities of shallow dynamic thermocapillary liquid layers", Phys. Fluids A **4** 11, (1992), pp. 2368–2381.
5. D. Villers, J. K. Platten, "Coupled buoyancy and Marangoni convection in acetone: experiments and comparison with numerical simulations", J. Fluid Mech. **234**, (1992), pp. 487–510.
6. P. Gillon, G. M. Homsy, personal communication, (1996).
7. M. Mundrane, A. Zebib, "Two- and three-dimensional buoyant thermocapillary convection", Phys. Fluids A **5** 4, (1992), pp. 810–818.
8. W. V. Kayser, J. C. Berg, "Spontaneous convection in the vicinity of liquid meniscuses", Ind. Eng. Chem. Fundam., **10** 3, (1971), pp. 526–529.

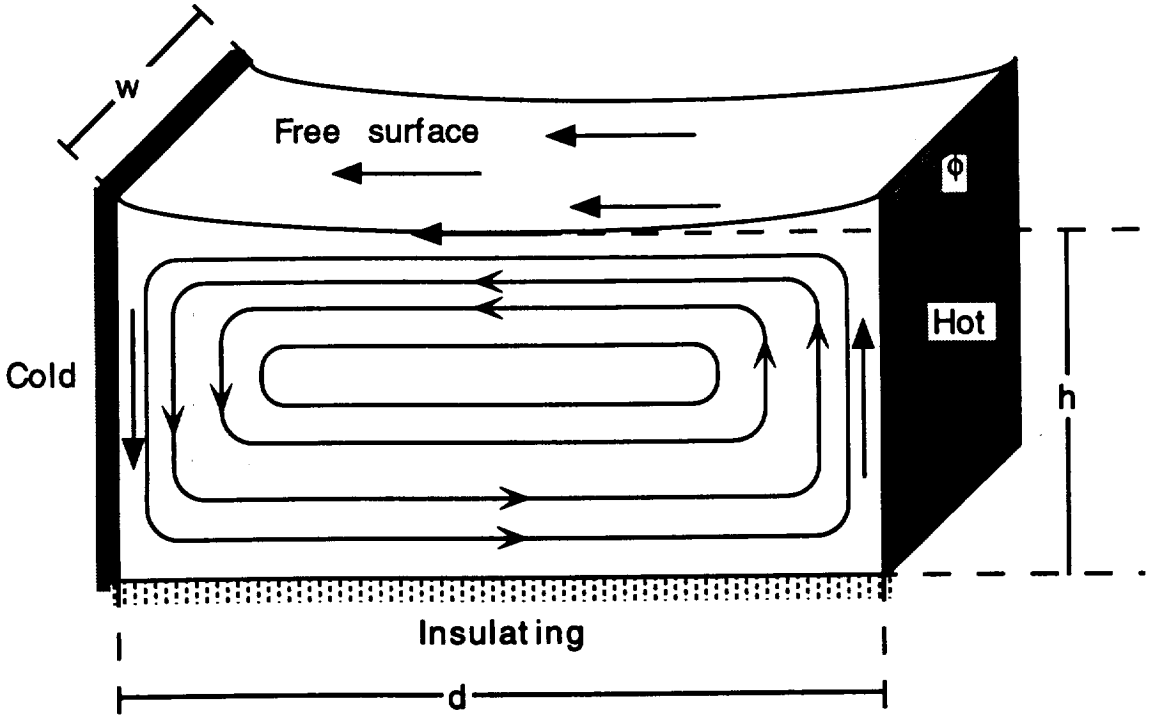

Figure 1: Schematic view of the geometry

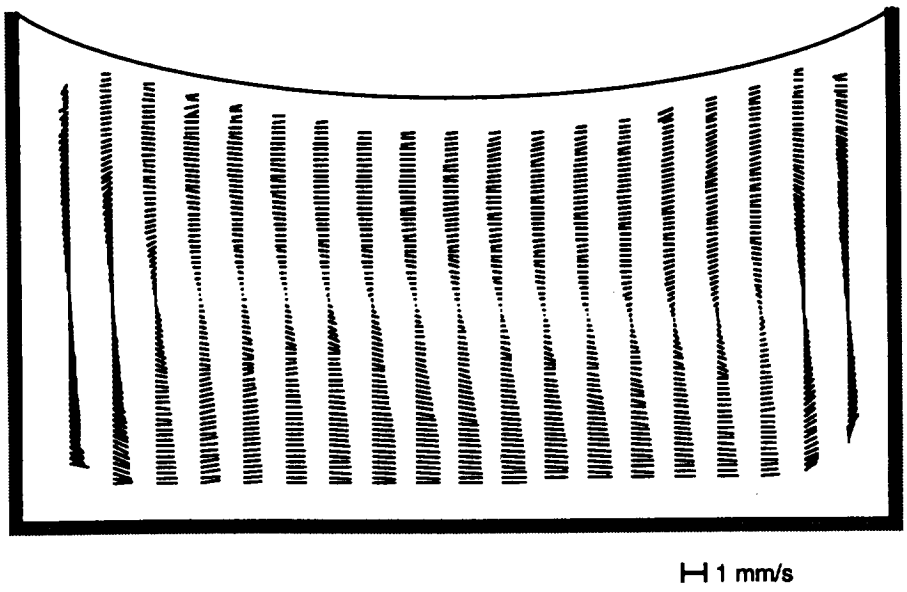

Figure 2: Velocity field on the center section of the cell, at A_x=1.81, Ma=7.67×10^4, Ra=1.31×10^5, G=3.10.

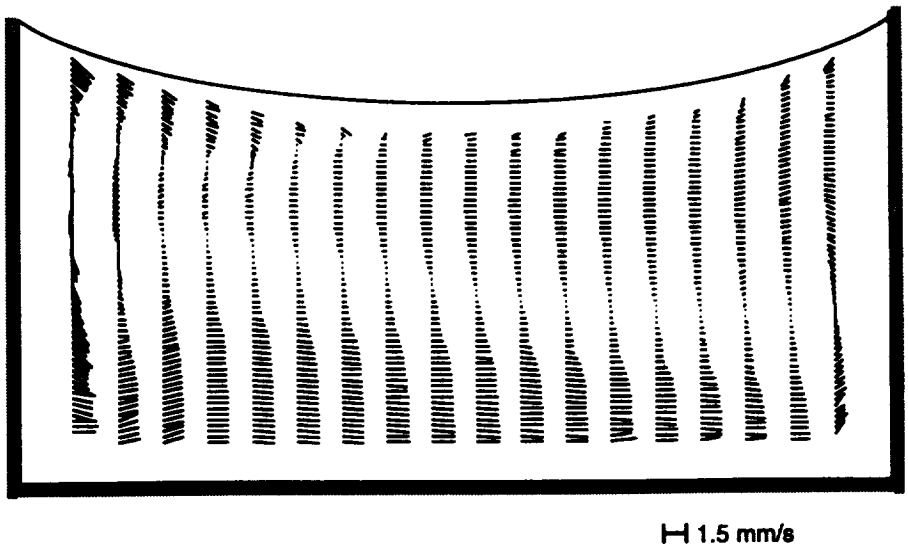

Figure 3: Velocity field on the center section of the cell, at A_x=2.35, Ma=3.44×10^5, Ra=2.71×10^5, G=1.85.

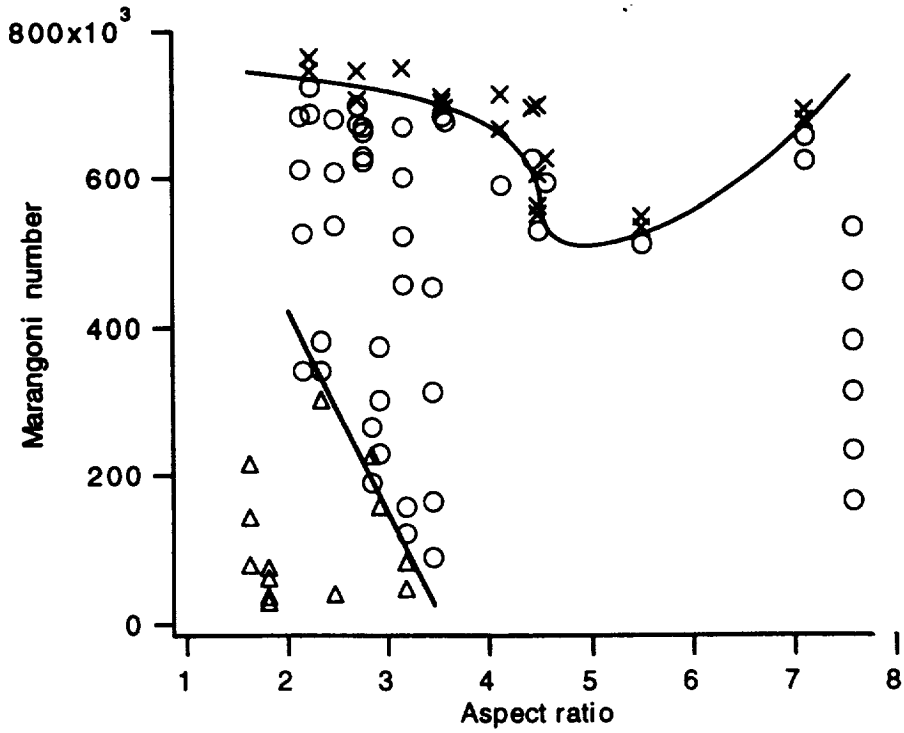

Figure 4: Overview of parameter space. Δ: steady 2-D flow, ○: steady 3-D flow, ×: oscillatory flow.